Diyala Journal of Engineering Sciences Vol. 12, No. 03, Septemper 2019, pages 55-64 ISSN 1999-8716
DOI: 10.24237/djes.2019.12307 eISSN 2616-6909

Synthesis and Optical Properties of CdS_xSe_{1-x} Semiconductor Nanomaterials by Chemical Vapor Deposition Method

Nadia M. Jassim

Department of Physics, college of science– Daiyla University – Baquba City 32001, Daiyla governorate, Iraq.
***corresponding author: email address:** *alaahadi18@yahoo.com, nadiajassim@sciences.uodiyala.edu.iq*

Abstract

Highly pure and crystalline CdS_xSe_{1-x} nanostructures have been successfully synthesized via Chemical Vapor Deposition (CVD) method, changing the components of x, in order to adjust the band gap of materials, and the relationship with the lattice constant. Using X-ray Diffraction (XRD) to characterize the phase structures and elemental compositions of the samples, and using Field Emission Scanning Electron Microscopy (FESEM) to observe the surface morphology of CdS_xSe_{1-x} nanomaterials and confirm the VLS growth mechanism. Using the High Resolution Transmission Electron Microscopy (HRTEM) and Selected Area Electron Diffraction (SAED) to analyze the crystal structure and the growth direction of the materials

Keywords: Chemical Vapor Deposition (CVD); Semiconductor nanomaterial; CdS; CdSe; Field Emission Scanning Electron Microscopy (FESEM); Resolution Transmission Electron Microscopy (HRTEM).

Paper History:-

(Received :23/1/2018; Accepted:14/5/2018)

Introduction

Due to the unique optical and electrical properties as well as the potential applications in microelectronic devices , the semiconductor nanostructures have attracted great attention of the scientific researchers. Specially, the typical II-VI semiconductor materials, such as Cadmium Sulfide (CdS) and Cadmium Selenium (CdSe) have important application prospect due to their optoelectronic performance, such as LEDs, nanolasers and optoelectronic detectors in the visible spectrum range. The solid solution CdS_xSe_{1-x} semiconductor nanostructure has many similar properties with its original binary compound CdS and CdSe. The flexibility of the CdS_xSe_{1-x} semiconductor nanostructure's band gap will also greatly enhance the ternary compound application value for optoelectronic devices [1,2]. One-dimensional semiconducting nanomaterials such as nanorods or wires, nanoribbons and nano whiskers are grown by vapor phase method. For example, II-Group VI semiconductors ZnS, ZnSe, SnO_2 and In_2O_3, Group III-V GaN, GaP, GaAs, etc. [3,4]. CdS is a very important and very practical Group II-VI direct band gap semiconductor compounds, at room temperature. The bandwidth of 2.42eV, with unique physical and chemical properties, is used as a solar cell window material. Material, at the same time has a high infrared transmittance, because of its excellent optical properties, in light absorption, photoluminescence, non-linear optics, photoelectric conversion photocatalysis and stimulated radiation and laser applications, etc., have a very wide range of research value CdS materials have many advantages, such as low overflow, high refractive index and mobility, chemical and thermal stability, high transmission rate and outstanding piezoelectric properties and so on, these properties make it in flat panel displays, field emitters, nonlinear optics, crystal tubes, photo detectors, optical waveguides, lasers and other devices have very clear advantages [5-11]. CdSe is also an important direct band gap group II-VI semiconductor compound, especially for visible light sensitive, has been widely used in photovoltaic cells, diodes and X-ray, light detectors and visible light detectors and other various photoelectric devices. The two solid solutions and the original binary compounds will have many very similar properties, its important performance parameters, for example such as lattice constant, forbidden band width, optical properties, luminescent color and so on will change continuously with the composition changes, Its bandwidth flexibility will also greatly enhance the value of this ternary compound in optoelectronic devices. Here, half conductor nanostructures CdS_xSe_{1-x} sets both optical properties such as extremely short response time, excellent non-linearity, etc [12]. Nature, in the optical communications, optical switches, optical signal processing applications such as tremendous potential. Therefore, you can use the simplest method of changing the ratio of the source materials adjusts the

change of the material composition while modulating the basic properties of the material, for example, Freely adjust its band gap, band structure, lattice constant, etc., for the choice of device materials provides a very great freedom and selectivity. Based on the above analysis, CdS_xSe_{1-x} semiconductor nanomaterials in the preparation process, by adjusting the reaction source material CdS and CdSe ratio, while studying the best reaction parameters (such as heating temperature, air flow size, pressure, the substrate bit set, holding time, heating rate, etc.) prepared high crystalline quality of CdS_xSe_{1-x} nano-materials, as well as the material ban the variation of the tape width with the source material composition is of great significance. At the same time, in the past about CdS, CdSe or most of the studies on the optical properties of CdS_xSe_{1-x} semiconductor nanostructures are based on single-photon excitation. Since Professor Qian Qian [13] and Prof. Marine W. [14] used two-photon excitation in the study of nanomaterials, resulting in very good the experimental results, the realization of the laser output, from which two-photon excitation has caused a great deal of scientific research workers Xing interest, so two-photon excitation has been greatly promoted. Two-photon excitation here refers to the excitation of photons less than the forbidden band width of the excited material; it can achieve the transition by absorbing two photons simultaneously.

Experimental Work

Experimental consumables and equipment

In our experiment, the following consumables including CdS (Cadmium Sulfide, powder, 99.995% trace metals basis), CdSe (Cadmium Selenide) and Au (Gold nanoparticles, 30nm diameter,OD1, stabilized suspension in citrate buffer) are all purchased from Aldrich. The substrate for the collection of nano materials is the n-type mono crystalline silicon wafer (single side polished) in the < 100 > direction provided by Zhejiang Crystal Optronics Co., Ltd. Our reagents mainly include the distilled water, the ethyl alcohol, the hydrogen peroxide and the sulfuric acid that are analytically pure. The carrier gas we've used is the 5% high purity argon gas (99.999%) mixed with H_2. Moreover, some routine lab consumables, such as the quartz boat and quartz tube (The external diameter is separately 50mm and 30mm) are also used in our experiment. Our compound vacuum gauge, F-5227 is produced by Chengdu Reborn Electronic Technology Co. , Ltd. The high vacuum metal oil diffusion pump is purchased from Chengdu Rankuum Machinery Co., Ltd and the two stage rotary vane vacuum pump, VRD-16 is provided by Zhejiang Overflying machinery Co., Ltd. Our horizontal tube furnace, Lindberg/Blue M with the model number of HTF55322C is made in USA. The material characterization instruments used in this experiment mainly include the field emission scanning electron microscopy (Abbreviated as SEM with the model number of Sirion 200, continuously adjustable with the accelerating voltage of 200V~30 kV. Specimens can be amplified by 40 times~400,000 times with the resolution up to 1.5 nm) produced by FEI company in Netherlands. Also our transmission electron microscopy (Abbreviated as TEM with the model number of Tecnai G2 20, the magnification of 25x – 1100000x and the resolution of 0.248nm (point) and 0.144nm (line)) is produced by FEI company from Netherlands as well. X-Ray diffraction (Abbreviated as XRD with the model number of XX'Pert PRO) is produced by PANalytical B.V. in Netherlands.

Nanowire preparation methods

In our experiment, the chemical vapor deposition (CVD) method is adopted to grow the nano materials. With this method, firstly we need to prepare the substrates for sample collection. For these purpose, cut the n-type mono silicon wafer with a diameter of 99.9 —100.3mm, a thickness of 505-545 μm in the <100> direction into slices in a size of 2x2 cm^2 with the diamond blade. After the cutting, clean the slices according to the standard procedure with the specific steps provided as below: (1) Open the door of the incubator and set the temperature to be 80ºC. (2) Immerse the silicon slices in the 80ºC piranha solution (H_2SO_4:30%H_2O_2 is 3: 1) for 1h and then clean them over and over again with distilled water after the cooling of the slices. (3) make an ultrasonic cleaning for 1h in the H_2O:NH_4OH:30%H_2O_2 solution (The ratio is 5:1:1). (4) Clean the silicon slices through distillation and then drip a drop of gold particle solution on each silicon slice. Make sure that the gold particle solution spreads all over the slice, which will then be placed into the oven for around 10 minutes of drying. Begin the growth experiment after the substrate has been prepared. In this experiment, we adopt the method of "smaller pipe within a larger pipe

Firstly, weigh a suitable amount of CdS and CdSe nano powder (according to a certain mixing ratio) in the quartz boat, which is placed in the middle of the tube. Then place the quartz boat that carries a substrate (keep the side coated with gold particles up) in the downstream of the airflow at a distance of 17~23cm away from the thermal center. the experimental system consists of the following three parts including the vacuum system, the heating system and the air flow control system. (1) The vacuum system mainly consists of the following three parts, including the mechanical pump, the metal oil diffusion pump and the cooling

water circulation. In this experiment, firstly we used the mechanical pump to exhaust the air in the cavity until the air pressure drops to 10-1Pa. Then start the cooling water circulation system and turn on the mechanical pump for around half an hour of preheating. When the cavity of the metal oil diffusion pump becomes hot, turn off the pre-inlet valve and turn on the high and low vacuum valves to realize deep deoxygenization in the cavity until the air pressure is as low as around $3x10^{-3pa}$. Then continue to exhaust the air for 10 minutes. After that, turn off the diffusion pump and turn on the pre-inlet valve for air washing. (2) The air flow control system. It mainly consists of the following two parts, including the flow meter and the high-purity gas (95% Ar+ 5%H). In the air-washing process, turn on the gas cylinder and adjust the flow meter to control the airflow rate, which generally is around 100sccm for approximately 1 hour. After that, set the airflow rate in the reaction process as per the experimental requirement in addition to the regulation of the reaction gas pressure. (3) The heating system. It mainly consists of the tube furnace as shown in figure 1 and the temperature controller. The temperature controller is used to set the heating rate and the heating temperature, which must be kept for a period of time. After that, turn off the thermostat and cool the quartz tube down to the ambient temperature naturally .

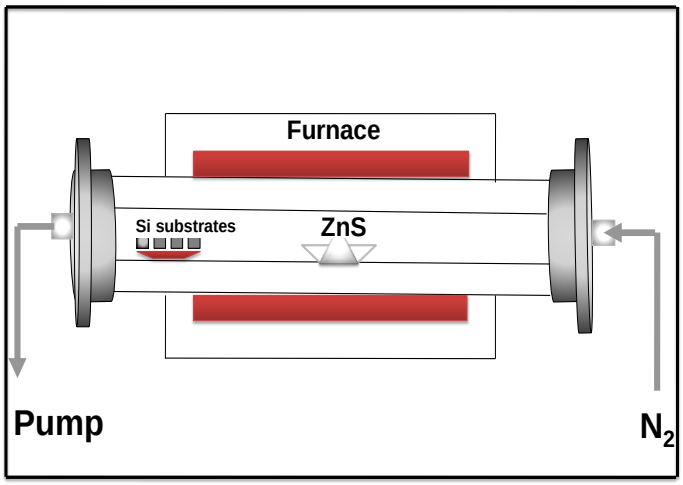

Figure1: Tube Furnace of Chemical Vapor Deposition system.

The X-ray diffraction (XRD) technology and the analysis

The composition and the structure of the material are the most basic factors that decide its physical property. However the application of the XRD technology makes it possible to obtain the information, such as the crystal phase structure and the elementary composition etc about the tested material. It's also called as the powder diffraction method [15], when the characteristic X-ray diffraction is used to obtain the diffraction pattern of the polycrystalline powder in addition to data characterization. With this method, the diffraction pattern of the polycrystalline powder is actually the overlapping effect of the various diffraction planes caused by numerous tiny crystal particles. This is because that with the incidence of the monochromatic X-ray upon the polycrystalline powder at a certain angle, there must be some small particles with some of their net planes conforming to the Bragg equation in the irregularly-arranged powder to give rise to the emergence of X-ray. It is also called as the qualitative phase analysis [16], when X-ray is used to make a judgment about what elements have constituted the tested sample according to the diffraction position on the sample and the intensity of the X-ray. The principle is that: The interplanar distance, d can be measured according to the angle and the position of every diffraction peak, while the relative intensity of the diffraction peak is the inherent characteristic of the tested material. Therefore no repetition will occur, as every group of crystal structures and the lattice constants correspond to every material on a one-to-one basis. Hence due to the correspondence between such a structure and constant with the diffraction angle and the diffraction peak intensity, it's possible to identify the crystal structure of the tested material according to the diffraction data.

Diyala Journal of Engineering Sciences Vol. 12, No. 03, Septemper 2019, pages 55-64 ISSN 1999-8716
DOI: 10.24237/djes.2019.12307 eISSN 2616-6909

Actually the comparison with the diffraction pattern for a given phase makes it possible to identify the various phases in an unknown sample. Therefore nowadays, people always make a one-to-one comparison directly with the JCPDS card or just search through the database on the computer. As shown in Figure 2,

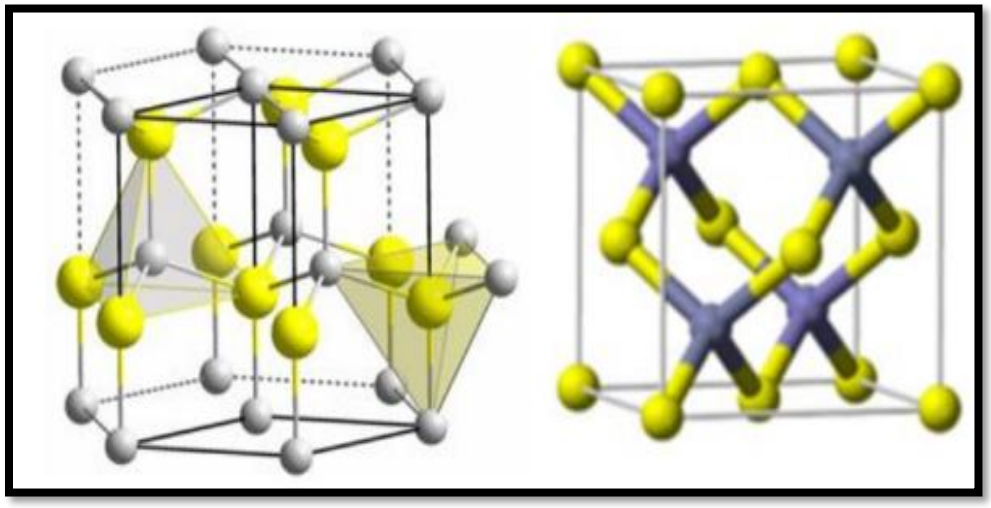

Figure 2: Crystal models of wurtzite and sphalerite

CdS_xS_{1-x} nano material can be grouped into two crystal types, wurtzite and sphalerite: In order to explain the crystal type of the nano structure that has been acquired in our experiment and the change law of the lattice parameters, we've utilized the XRD to make a characterization of the CdS_xS_{1-x} nano material with different S/Se ratios grown in our experiment. The analysis on the test result is as below ：

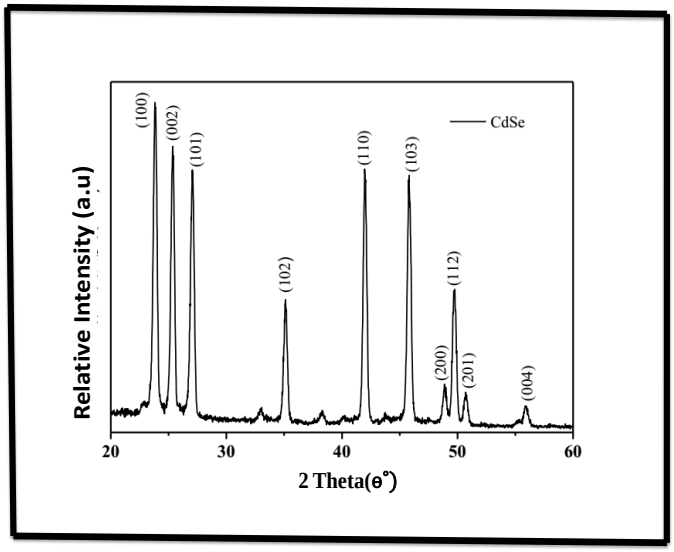

Figure 3: X-ray diffraction pattern of CdSe

Figures 3 and 4 are XRD patterns of pure cadmium selenide and pure cadmium sulfide nanowires, respectively, of a wurtzite structure, and respectively, with the corresponding standard card data, at the same time, two sets of data will be found, compared to the X-ray pattern of cadmium selenide, the peak position of CdS should be greater, at the same time, the more sulfur-containing components are present material, the corresponding peak position angle is bigger. Figure 5 (b) - (d) are XRD patterns of selenium-cadmium nanomaterials, and (a) and (d) comparison found that the XRD patterns of the selenium cadmium sulfide nanostructures and wurtzite cadmium sulfide and cadmium selenide images of large are the same and the peak angle is in between, indicating that the material structure is also hexagonal wurtzite and is sulfur and selenium two elements of the results Figure 4 shows the X-ray diffraction pattern of nano crystalline CdSe. Use X'Pert High Score Plus software analysis, we can determine the growth of nano-materials for the hexagonal structure, namely wurtzite structure, and six-phase CdS standard card Tablets (ICDD: 77 - 0046, a = 0, 4299 nm, c = 0.7010 nm) are consistent. No other diffraction peaks appear in the figure, this shows that the purity of the product is high, and the peak of the diffraction peak indicates that the product has well crystalline.

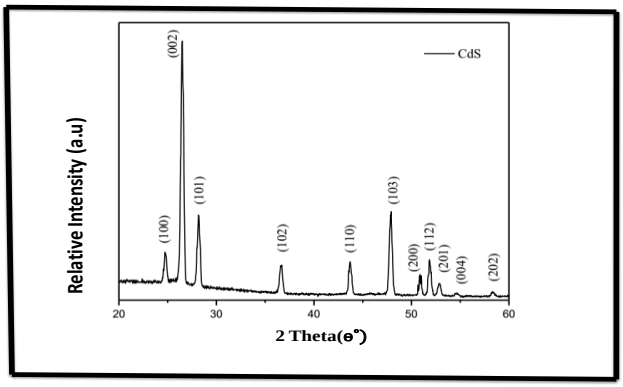

Figure 4: XRD patterns of CdS nanomaterials

Figure 4 shows the X-ray diffraction pattern of CdS nanomaterials. Use X'Pert High Score Plus software analysis, we can determine the growth of nano-materials for the hexagonal structure, namely wurtzite structure, and six-phase CdS standard card Tablets (ICDD: 41-1049, a = 0,4141 nm, c = 0.6720 nm) are consistent. There are no other examples in the picture Peaks, indicating the purity of the product, and the diffraction peak is sharp, said product crystalline. In addition, the (002) peak is particularly sharp so the material's preferred growth direction is (002). Figure 5 shows the X-ray diffraction pattern of the product CdSxSe1-x, where line (a) is the XRD of CdS grown (E) line for the growth of CdSe XRD patterns, we can see from Figure 5: (1) x changes from 0 to 1, which can be seen from the XRD pattern. The position of each diffraction peak increases with the increase of x, angle movement, according to the diffraction formula [17].

$$2dsin\theta = n\lambda \quad (1)$$

Note that as component x is constantly changing and unchanged and the position of the diffraction peak shifts, indicating the same d interplanar distance changes, that is, the semiconductor nano crystalline material CdSxSe1-x lattice constant changes. So, with x, the corresponding peak moves to a large angle, $\boldsymbol{\theta}$ increases, sin $\boldsymbol{\theta}$ increases, $\boldsymbol{n\,\lambda}$ remains the same, then $\boldsymbol{d}$ decreases [17]

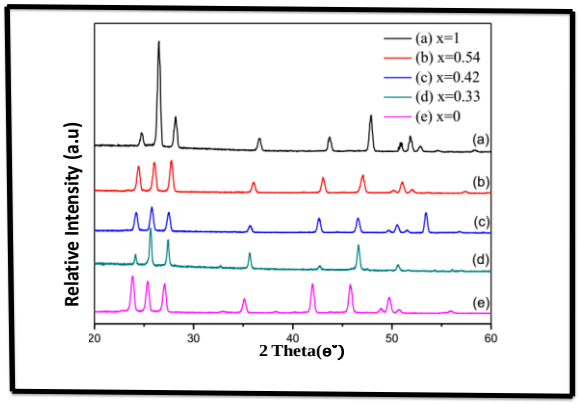

Figure 5: X-ray diffraction pattern of CdS_xSe_{1-x}

d value analysis of two different x-component crystal planes, (002) plane, from CdS to CdS0.33Se0.67, d_{002} values from 0.3360nm to 0.3451nm, (112) plane, from CdS to CdS0.33Se0.67, d_{112} value from 0.1763nm increase to 0.1796nm. This is because the semiconducting nanomaterial CdS_xSe_{1-x} part of the ionic radius Se^2 ion (R = 0.198 nm) replaced S^{2-} ions with small ionic radius (r = 0.184 nm), and the proportion of unit cell with Se^{2-} increase and expansion, resulting in increased spacing between its surface. The shape of each diffraction spectrum of CdS_xSe_{1-x}(x= 0 ~ 1) is similar, which shows that the two kinds of fiber zinc the structures of CdS and CdSe form a solid solution semiconductor CdS_xSe_{1-x}, which keeps the structure of wurtzite unchanged. the crystal structure, dimensions and surface and energy band structure of semiconductor nanomaterials determine its excellent properties rational properties, in which the crystal structure of the semiconductor material itself is similar to the band structure. Solid solution semiconductor is a very important class of semiconducting materials that cannot be obtained by artificially synthesizing materials as needed of the band structure or other properties, the II-VI group, III-V or IV-VI two crystal structures similar to the binary the semiconductor materials are mixed together to synthesize a new composite semiconductor structure and performance between the two, like such ternary semiconductor structure, can be called infinite solid solution. The most prominent feature of solid solution is that it can be changed crystal composition ratio to change here to grow our CdS_xSe_{1-x}, for example, the solid solution lattice constant a (x) and CdS, CdSe lattice constant a_{CdS}, a_{CdSe} approximately satisfy the linear relationship

$$a(x) = xa\ CdS + (1-x)aCdSe \quad (2)$$

The famous Vegard's law is quoted here [18]. The experimental lattice parameters corresponding to the following table and the corresponding band width changes to be:

$$E_g(x) = (1\text{-}x)\ E_{gCdSe} + x[\ E_{gCdS}\text{-}b] + bx^2 \quad (3)$$

Where, b is the bending constant [18], which has little to do with the size of component x. Because of the crystal structure of CdS and CdSe two species of compounds with the same band gap, then the solid solution CdS_xSe_{1-x} band gap will be with the components approximately from the CdS even continued changes to CdSe. In this way, we can arbitrarily combine the two materials as needed to adjust the forbidden band width.

Table 1: CdS_xSe_{1-x} crystal components of different components

Composition	Crystal type	Lattice constant	ICDD serial number
CdS	Hexagonal	a= 0.4141nm, b= 0.6720nm	41-1049
$CdS_{0.54}Se_{0.46}$	Hexagonal	a= 0.4180nm, b= 0.6850nm	89-3682
$CdS_{0.42}Se_{0.58}$	Hexagonal	a= 0.4215nm, b= 0.6872nm	50-0720
$CdS_{0.33}Se_{0.67}$	Hexagonal	a= 0.4233nm, b= 0.6883nm	50-0721

CdSe	Hexagonal	a= 0.4299nm, b= 0.7010nm	77-0046

Characterstics of CdS_xSe_{1-x} Nanomaterials

The CdS_xSe_{1-x} nanowire grown in our experiment varies in diameter according to the different positions with the source material separately through the SEM, FETEM and EDS analysis. Figure 6 shows an FESEM (field emission scanning electron microscopy) image of the CdS_xS_{1-x} nanowire grown in our experiment. A scanning electron microscope mainly consists of the following six systems, including the electro-optical system, the vacuum system, the scanning system, the signal detection and amplification system, the image display and record system and the power supply system. The working principle is: Use an electronic gun to emit electrons with energy ranging from 5 to 35keV. Then take the crossover spot as the electron source to obtain an incident electron beam with a certain energy and a certain beam intensity with the diameter of the beam spot at 5nm or less than 5nm under the effect of the accelerating voltage after the zoomed out and focused processing through the two-stage condenser and the objective lens. Driven by beam scanning in circles, the incident electron beam will scan the surface of the sample in grids according to a certain chronological and spatial order. When the incident electrons are emitted onto the surface of the sample, the focused electron beam will interact with the specimen to generate various physical signals (such as the secondary electrons, the backscattered electrons and the X-ray etc). With the difference in the surface morphology of the samples, the intensity of the generated signals varies as well. After measured by the corresponding detection system, all of these electronic signals will be amplified and transformed into voltage signals, which will then be inputted into the kinescope grid after video amplification. Then modulate the tube brightness in synchronous scanning to obtain a secondary electron image that can reflect the surface of the specimen. Furthermore, we can use the energy dispersive X-ray spectrum (EDS) installed in the scanning electron microscope to determine the specific elemental distribution and the composition of the sample. In this experiment, we directly place some materials with good electro conductibility into the sample cell to observe the surface topography of the samples. However for those materials with poor electro conductibility, it's necessary to perform metal spraying on the surface of the samples before the observation. In the SEM test, we can observe that there are lots of super-long nanobelts and nanowires with a diameter up to hundreds of nanometers distributed uniformly on the silicon wafer. The surface of all of these nanobelts and nanowires is very uniform. Table 2 shows the comparison on the growth parameters provided in Figure 6(a) and Figure6 (b) as below. It indicates that the growth temperature, the holding time, the airflow rate and the growth pressure are the same in both figures.

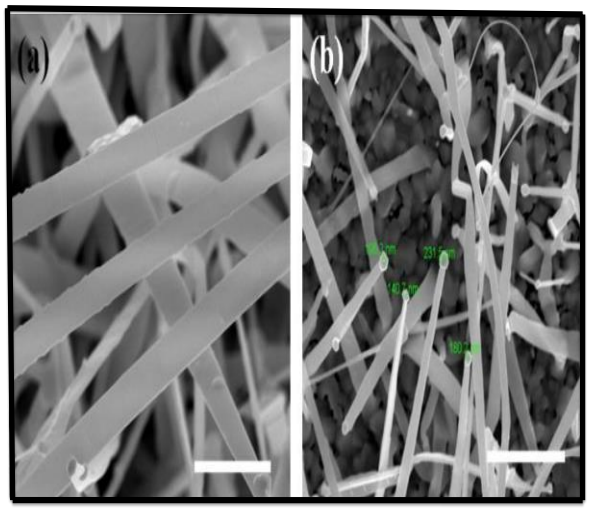

Figure 6: SEM image of selenium cadmium sulfide nanowire, scale 2μm

Table 2: Growth parameters of selenium cadmium sulfide nanowires

Parameter	Temperature/ ˚C	Holding time/h	Airflow size /SCCM	Air pressure /Torr	Distance from source/Cm
(a) Figure	820	1	150	150	19-21
(b) Figure	820	1	150	150	22-23

In addition, it can be clearly observed from the SEM of Figure 6 (b) that there is a small particle on the top of the nanowire, as shown 6 middle right. Presumably, we consider the catalyst gold particles added, and follow the above description VLS growth mechanism. As shown in Figure 7, the catalyst gold particles melt into one small droplet at high temperature, with the CdS and CdSe vapor is brought to the silicon substrate by a mixed gas of Ar and H2 and undergoes a series of chemical reactions to form selenium sulfur-cadmium ternary alloy, when the surface of Au droplets in the selenium and cadmium vapor over-saturated, the selenium and cadmium nuclei in the Au / Si surface formation. With the continuous deposition and overflow of steam, a selenium-cadmium nanowire with gold nano particles on the top was formed
.

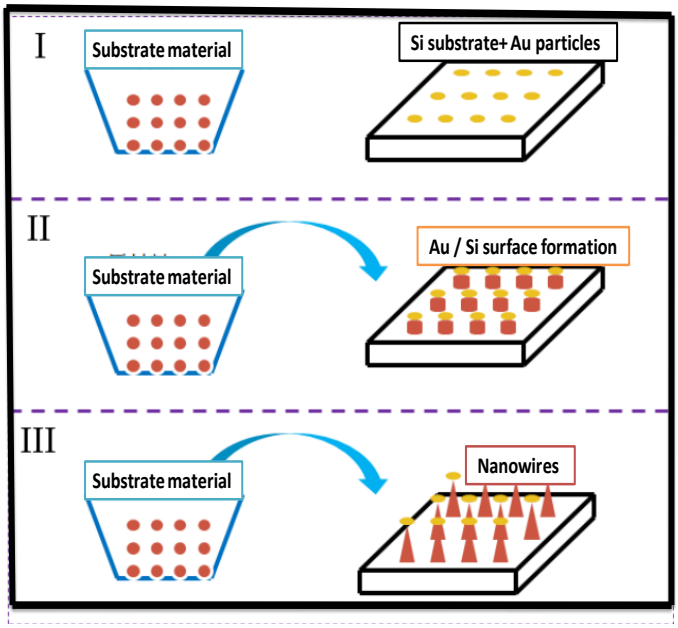

Figure 7: VLS mechanism of selenium-cadmium nanowires

The only difference lies in the distance from the source position. In the left image, the diameter of the nanowire is around 500nm. However in the right image, the diameter is around 150nm. Therefore it's obvious that the transmission electron microscopy (TEM) that has been mainly applied in the study of the nano technology can be used to measure the distance between the substrate and the source material within the growth scope due to the extremely high resolution that is up to 0.2nm. With a wide application in the nano domain, TEM has been mainly used for the morphological observation and the study of the crystal structure, the particle size distribution and the forms of the nano materials. TEM mainly consists of three parts, including the electro-optical system, the vacuum system and the electronics system. Among all of these three parts, the electronics system constituted by the illuminating system, the imaging system and the observing system is one of the most important parts in the TEM. The vacuum system is an important guarantee to secure the stability of the electron-beam current, and prevent the samples from being contaminated. Also it's an important basis and guarantees to avoid the presence of lens flare and the improvement of the substrate. As to the electronics system, it's used to provide the power supply and control the system. In addition to facilitating the analysis on the phase morphology, TEM can also be used to generate an electron diffraction pattern, where every spot represents a crystal cluster. As different

electron diffraction patterns correspond to different material structures, and then they can be used to analyze the phase structure of the material. The above analysis reveals that with the indexing of every spot in the diffraction pattern, the crystal plane indices can be determined as well. Then according to the standards manual, it's feasible to find out the relevant phases or make an analysis on the properties of the tested materials including the crystal symmetry, the Bragg type and the lattice constant etc. Figure 8 shows the HRTEM image of the CdSexS1-x nanobelt and the inset selected-area electron diffraction (SAED) pattern. It further verifies the mono crystalline characteristic of the CdSexS1-x nano material with a spacing of 0.686nm between the relevant lattices in the [002] direction. Also this figure shows that the tested nanobelt has grown along the [110] direction, while the corresponding nano comb has grown vertically in the [002] direction. The ESD shown in Figure 8 (d) proves that the nanobelts and nano combs that have been obtained in our experiment are composed of CdSexS1-x.

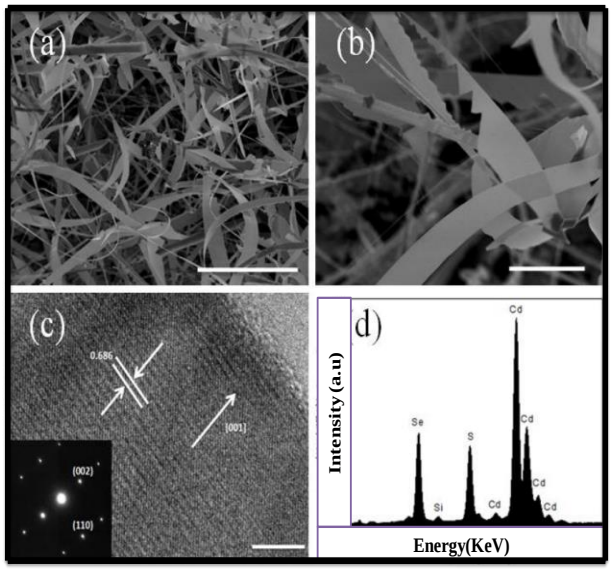

Figure 8 (a) and (b) are different resolution SEM images of selenium-cadmium-sulfur nanobelts with scales of 20 μm and 4 μm, respectively. Figure 8 (c) The HRTEM image of selenium-sulfur selenide nanoribbons, the illustration is SAED, the scale is 5nm; Figure 8 (d) EDS spectra of selenium and cadmium. As can be seen from Figures 8 (a) and (b), using a mixed powder of CdS and CdSe as a starting material, several tens micron long ribbon. At the same time, it can be seen from Figure 8 (a) that the ribbons are very dense; indicating the production of selenium, cadmium and cadmium high, purity is higher. As can be seen from the higher resolution figures 8 (b), the side edges of the ribbons are conspicuous serrated, the surface is very smooth, about 200 ~ 800nm tooth width, and gradually reduced to a tip. Based on this for some observations, we will refer to these toothed nanoribbons as pointed nano combs. Figure 8 (c) for the selenium cadmium sulfide nanobelts HRTEM and selected area electron diffraction (SAED) maps in the inset, further confirming the selenium-sulfur nanomaterials, and the lattice spacing corresponding to [002] direction is 0.686 nm. In this figure, the measured square of the growth of the nanoribbons in the [110] direction, the growth direction of the corresponding dentate nano combs is perpendicular [002]. From Figure 8 (d) EDS spectrum can prove that we have nanobelts and dentate nanoribbons composition of selenium and cadmium.

Conclusion

This work focuses on the verification of the structural characteristics of the grown materials through various material characterization methods. Firstly, it introduces the consumables and the experimental devices required in this experiment. Then with the introduction of the growth method, which is also the chemical vapor deposition method adopted in this experiment, this work makes a detail illustration on the experimental procedure and the three major parts in the experimental system. After that, it introduces the principle of the X-ray diffraction technology and analyzes one by one the phase structure and the elementary composition of the nano materials prepared in this experiment with different parameters. It proves that the nano materials grown in this experiment are purely composed of CdSeS with high degree of crystalline. it verifies the variation of

lattice constants for the ternary compounds with different S/Se ratios. Meanwhile, with the adoption of the FESEM to observe the surface topography of the sample, this study makes a comparison on the changes in the morphology of the outcome under the same experimental parameters (including the growth temperature, the holding time, the airflow rate and the reaction gas pressure) on the condition that only the distance between the substrate and the source position is different. Also, it illustrates that our nano material has been grown based on the VLS growth mechanism introduced as above. Finally, with the aid of the high-resolution TEM and according to the SAEDP and the energy spectrum analysis result, this work verifies that the tested sample is constituted by mono crystalline CdSeS with ternary nanostructure. Also the nanobelt grows along the [110] direction and the corresponding dentations nanostructure that is vertical to the nanobelt, grows along the longitudinal axis in the [002] direction.

References

[1] Li Y., Qian F., Xiang J., et al. Nanowire electronic and optoelectronic devices. Mater. Today, 2006, 9(10): 18-27.
[2] Y. Zhang, J. Cryst. Single-crystal gallium nitride nanotubes. Nature2016, 422, 599-602.
[3] R M. Davidson, R. Wiacek,B. A. Korgel. Supercritical Fluid−Liquid−Solid Synthesis of Gallium Phosphide Nanowires,Chem. Mater. 2015,17,230.
[4] S. R. Niranjan, S. Kittitat, Y. Yang, R. Grimm, R. Michiels, M. Zacharias,J. Phys.Chem. C 2010,114,10323.
[5] Zhang M., Zhai T. Y., Wang X., et al. Carbon-assisted morphological manipulation of CdS nano structures and their cathode luminescence properties. J Solid State Chem, 2009, 182 (11): 3188-3194.
[6] Fan X., Zhang M. L., Shafiq I., et al. Bicrystalline CdS nanoribbons. Cryst Growth Des, 2009, 9 (3): 1375-1377.
[7] Lin Y. F., Song J., Ding Y., et al. Alternating the output of a CdS nanowire nanogenerator by a white-light-stimulated optoelectronic effect. Adv Mater, 2008, 20 (16): 3127-3130.
[8] Zhai T. Y., Gu Z. J., Zhong H. Z., et al. Design and fabrication of rocketlike tetrapodal CdS nanorods by seed-epitaxial metal-organic chemical vapor deposition. Cryst Growth Des, 2007, 7 (3): 488-491.
[9] Lin Y. F., Song J., Ding Y., et al. Piezoelectric nanogenerator using CdS nanowires. Appl Phys Lett, 2008, 92 (2): 022105.
[10] Zhai T. Y., Fang X. S., Li L., et al. One-dimensional CdS nanostructures: synthesis, properties, and applications. Nanoscale, 2010, 2 (2): 168-187.
[11] Ma R. M., Wei X. L., Dai L., et al. Synthesis of CdS nanowire networks and their optical and electrical properties. Nanotechnology, 2007, 18 (20): 205605.
[12] Li H. Q., Wang X., Xu J. Q., et al. One-dimensional CdS nanostructures: A promising candidate for optoelectronics. Adv Mater, 2013, 25 (22): 3017-3037.
[13] Zhang C. F., Dong Z. W., You G. J., et al. Multiphoton route to ZnO nanowire lasers. Opt Lett, 2006, 31 (22): 3345-3347.
[14] Khitam S. Shaker., SYNTHESIS AND CHARACTERIZATIONS OF SILVER NANO PARTICLES USING CHEMICAL REACTION METHOD. Diyala Journal of Engineering Sciences, Vol. 09, No. 01, March 2016.
[15] Amin Daway Thamir, Adawiya J. Haider, Ghalib A. Ali. Deposition of Tio2/Pt Composite Particles Using Pulsed Laser Deposition Technique. Diyala Journal of Engineering Sciences, Vol. 09, No. 03, September 2016.
[16] McPherson A. The Growth and Preliminary Investigation of Protein and NucleicAcid Crystals for X-ray Diffraction Analysis[J]. Methods of Biochemical Analysis,Volume 23, 1976: 249-345.
[17] Liu Yuehui, Liu Ping. X- Ray diffraction analysis principle and application [M]. Beijing; Chemical Industry Press, 2003.10.
[18] Deng Zhijie, Zheng Ansheng. Semiconductor materials North learn Press,2004.10 a 67.